

Electronic Supplementary Information

Hydrogen bond and lifetime dynamics in diluted alcohols

Evgeniia Salamatova^a, Ana V. Cunha^a, Keisuke Shinokita^{a§}, Thomas L. C. Jansen^a,
and Maxim S. Pshenichnikov^{*a}

^aZernike Institute for Advanced Materials, University of Groningen, 9747 AG Groningen, The Netherlands

[§]Current address: Institute of Advanced Energy, Kyoto University, Uji, Kyoto 611-0011, Japan

*e-mail: m.s.pchenitchnikov@rug.nl

S1. Determination of the solution concentration range

Analysis of absorption spectra provides the concentration range from which the alcohol molecules tend to form clusters. Fig. S1 shows the absorption spectra in the spectral range of the OH-stretching mode of all studied alcohols at different molar ratios between alcohol and acetonitrile (MeCN). All obtained spectra show a strong absorption peak at $\sim 3535\text{ cm}^{-1}$ corresponding to the OH-stretching mode¹. The frequency shift of the OH stretching mode of $\sim 200\text{ cm}^{-1}$ to blue in comparison to the alcohol clusters and bulk alcohols^{1,2} indicates that the alcohol molecules stay well separated at the lowest concentration. However, with the increase of concentration, a red shoulder at $\sim 3450\text{ cm}^{-1}$ begins to develop. Following Farwaneh *et al.*¹, this shoulder is ascribed to absorption of coexisting cyclic alcohol trimers (3450 cm^{-1}) and complexes (3450 cm^{-1}), which consist of one MeCN and two alcohol molecules, because HBs between them are stronger than those between the alcohol and MeCN molecules.

To determine the molar ratios where the alcohol molecules are separated, we plot in Fig. S2 the dependence of OD on the alcohol-acetonitrile molar ratio at the main peak frequency ($\sim 3535\text{ cm}^{-1}$) and at the frequency which corresponds to absorptions of alcohol oligomers (3400 cm^{-1}). The dependence at 3400 cm^{-1} is quadratic at low molar ratios as expected from bi-molecular interactions. Later it becomes linear which indicates that the dimers concentration is saturated. The inflection point between the two regimes varies from 0.03 to 0.05 for the alcohols studied (0.03 for methanol, 1-propanol, and tert-butanol, 0.04 for ethanol, 1-butanol and 2-methyl-1-propanol, and 0.05 for 2-propanol and 2-butanol). For further experiments the molar ratio of 0.03 was chosen as a compromise between

unwanted clusterization, the signal-to-noise ratio and alcohol-acetonitrile relative contribution to the 2D IR signals.

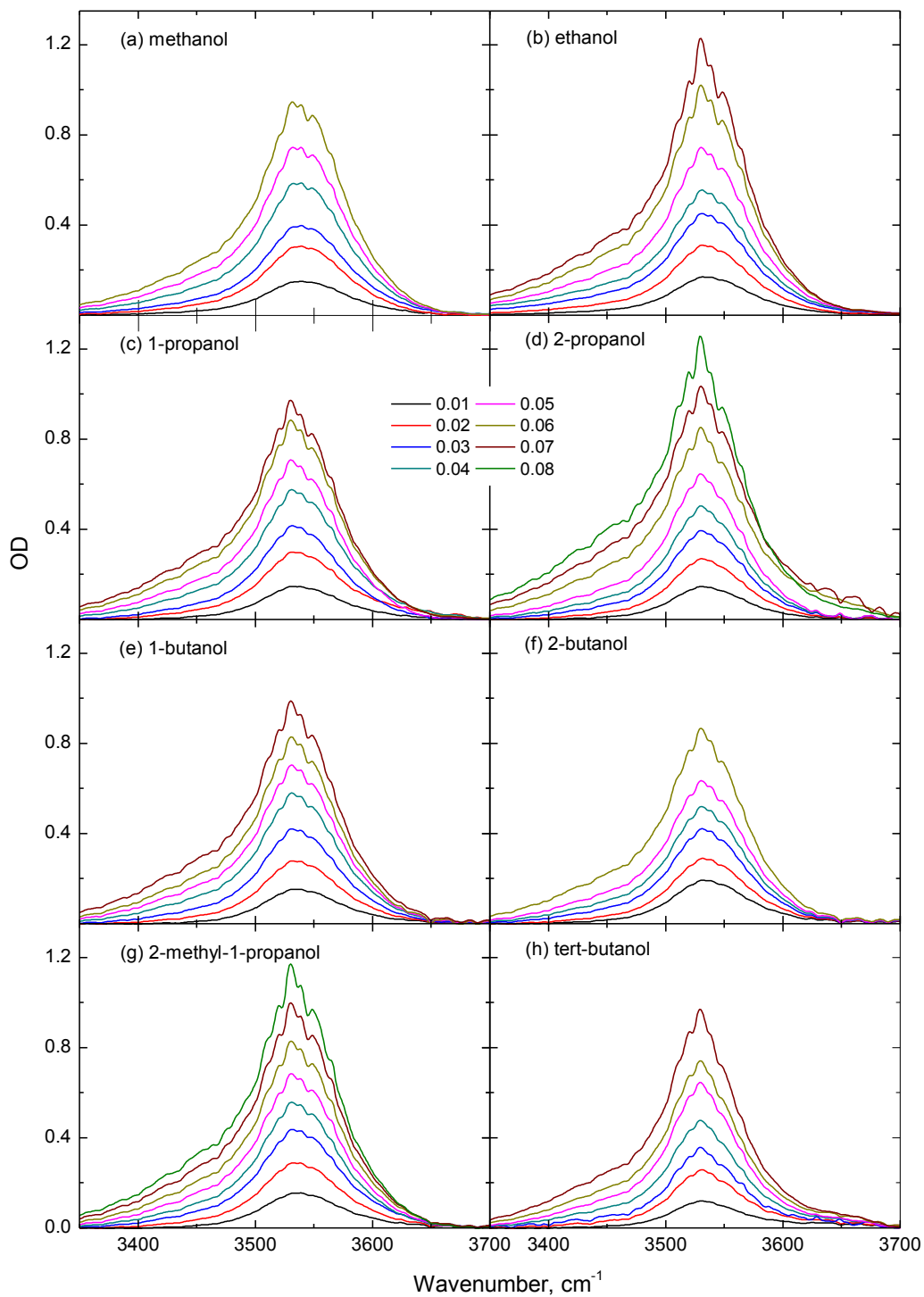


Fig. S1 Linear absorption spectrum of the OH-stretching region of (a) methanol, (b) ethanol, (c) 1-propanol, (d) 2-propanol, (e) 1-butanol, (f) 2-butanol, (g) 2-methyl-1-propanol and (h) tert-butanol dissolved in MeCN. Molar ratios of alcohol to MeCN are shown in the legend. Sample thickness is 100 μm .

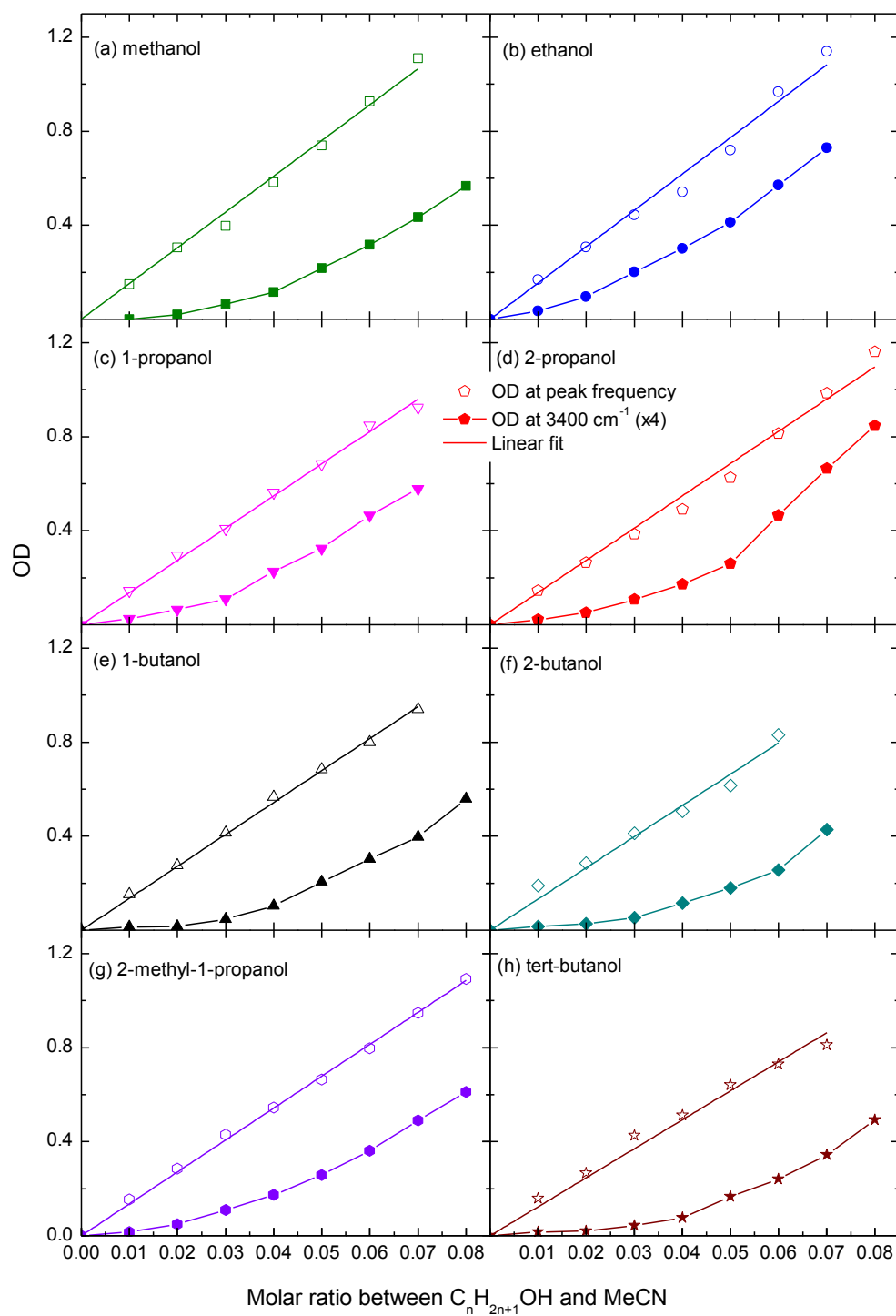


Fig. S2 Dependence of OD on the alcohol-acetonitrile molar ratio at the frequency OH-stretching mode (3535 cm^{-1}) and at 3400 cm^{-1} for all studied alcohol solutions: (a) methanol, (b) ethanol, (c) 1-propanol, (d) 2-propanol, (e) 1-butanol, (f) 2-butanol, (g) 2-methyl-1-propanol and (h) tert-butanol.

S2. Absorption spectra of the samples

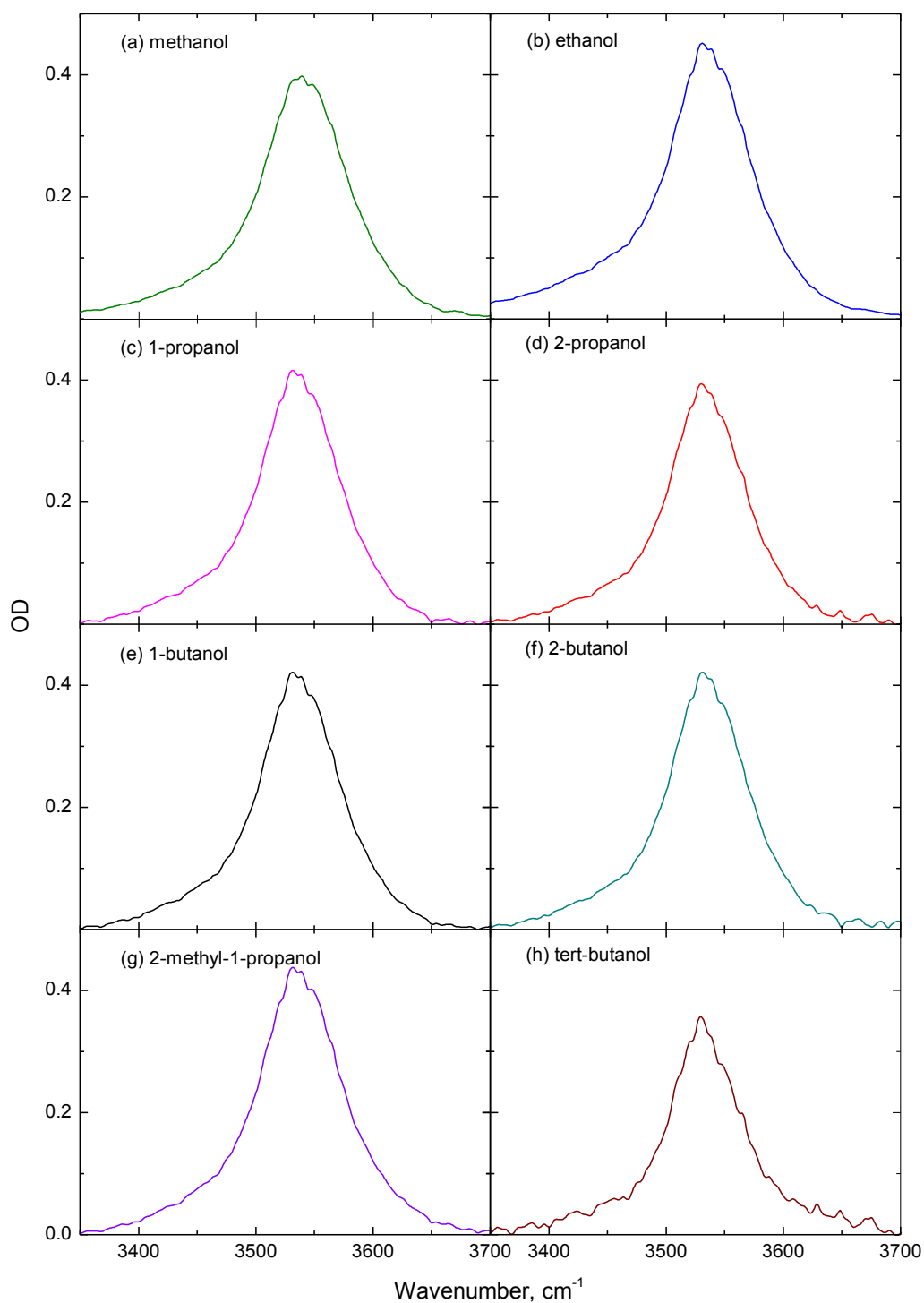


Fig. S3 Linear absorption spectrum of solutions used in pump-probe and 2D experiments. The molar ratio of alcohols to MeCN is 0.03 and the spectra are shown in the OH stretching region for (a) methanol, (b) ethanol, (c) 1-propanol, (d) 2-propanol, (e) 1-butanol, (f) 2-butanol, (g) 2-methyl-1-propanol and (h) tert-butanol dissolved in MeCN.

S3. Central frequency and width of absorption spectra

To determine the central position of the absorption peaks (Fig. S4 (a)), its top part at 80% of the maximum level, was fitted with a Gaussian function. The full width at half maximum (FWHM) values were calculated directly from the absorption spectra (Fig. S4 (b)). Neither value shows a strong dependence on the size of the alkyl chain group (Fig. S4); however, both central frequencies and widths tend to decrease with an increase of the size of the alkyl chain. In contrast, the calculated central frequencies increase (albeit slightly) while the spectral widths are hardly changed with the increase of the size of the alkyl chain group. This signifies that the classical force fields used are not fully optimized for this type of modelling.

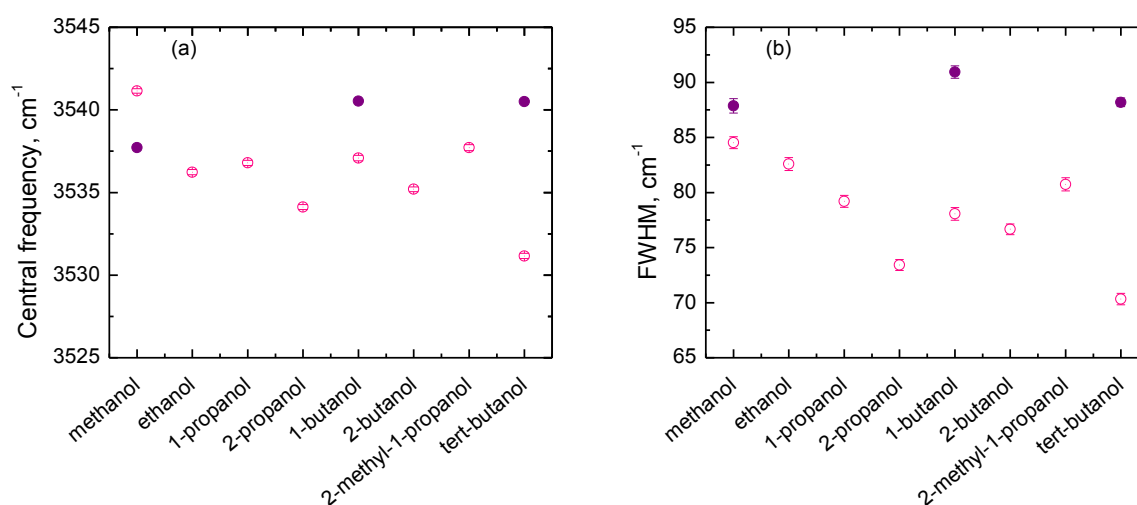


Fig. S4 (a) Central frequencies and (b) full width half maximum (FWHM) values of the experimental (open circles) and simulated (filled circles) spectra for all studied alcohols.

S4. Pump-probe

The pump-probe transients at the frequency of maximum bleaching (3535 cm^{-1}) and induced absorption (3370 cm^{-1}) with fits and isotropic transient absorption spectra at different delay times and are shown in Fig.S5 and Fig. S6, respectively, for all studied alcohols. At short delay times, the isotropic transient spectra are mostly dominated by bleaching (related to $|0\rangle \rightarrow |1\rangle$ transition) with the peak at $\sim 3535 \text{ cm}^{-1}$ and an induced absorption band (related to $|1\rangle \rightarrow |2\rangle$ transition) at the low frequency side at $\sim 3370 \text{ cm}^{-1}$. The anharmonicity of 170 cm^{-1} was calculated as a frequency shift between the peaks of induced absorption and bleaching/simulated emission.

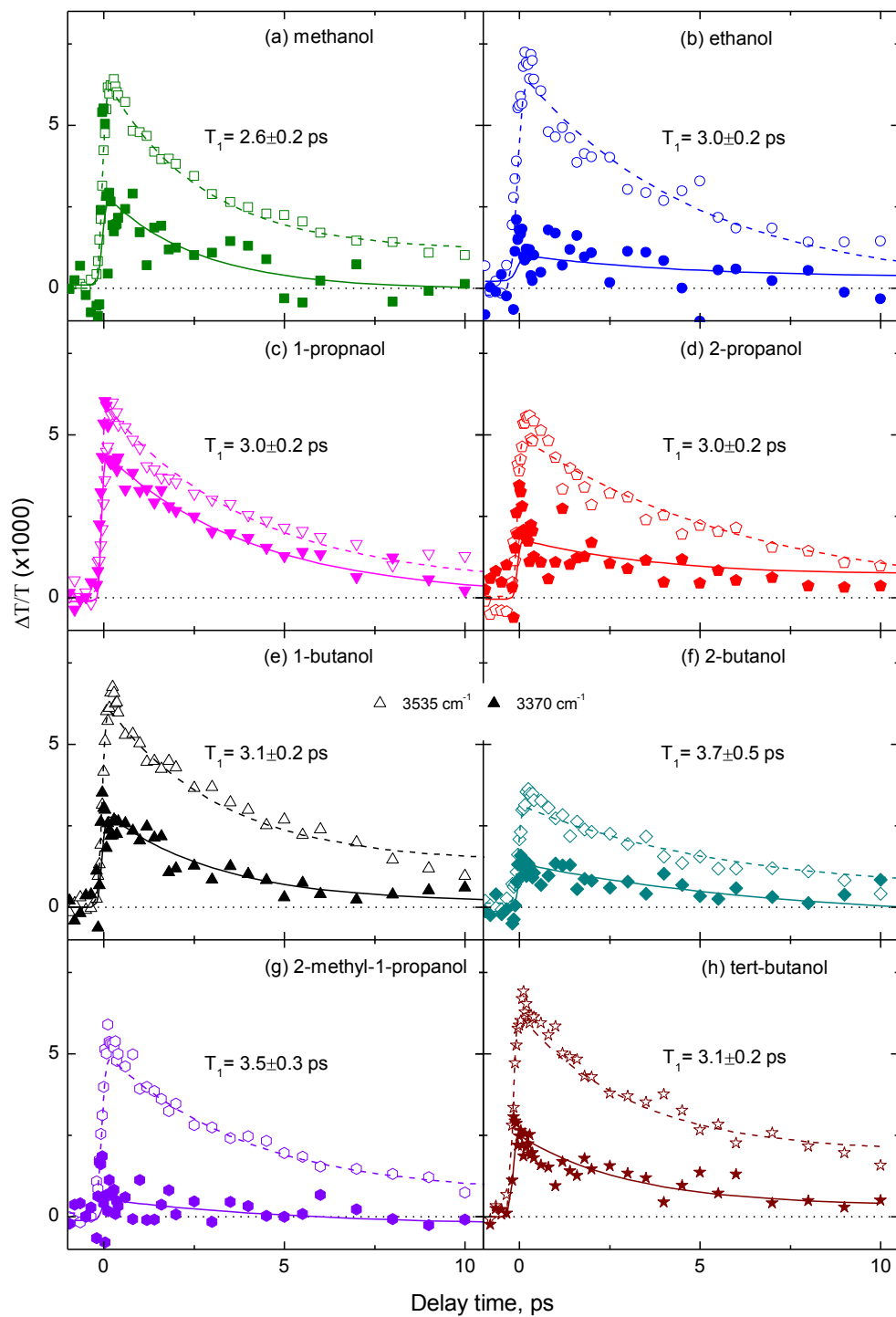


Fig. S5 Experimental transients (symbols) at bleaching/stimulated emission (3535 cm^{-1} , open circles) and induced absorption (3370 cm^{-1} , filled circles, the sign is inverted) regions for (a) methanol, (b) ethanol, (c) 1-propanol, (d) 2-propanol, (e) 1-butanol, (f) 2-butanol, (g) 2-methyl-1-propanol and (h) tert-butanol diluted in MeCN. The fits obtained from a kinetic model (Fig. S7) are shown by the lines with the corresponding lifetimes T_1 indicated.

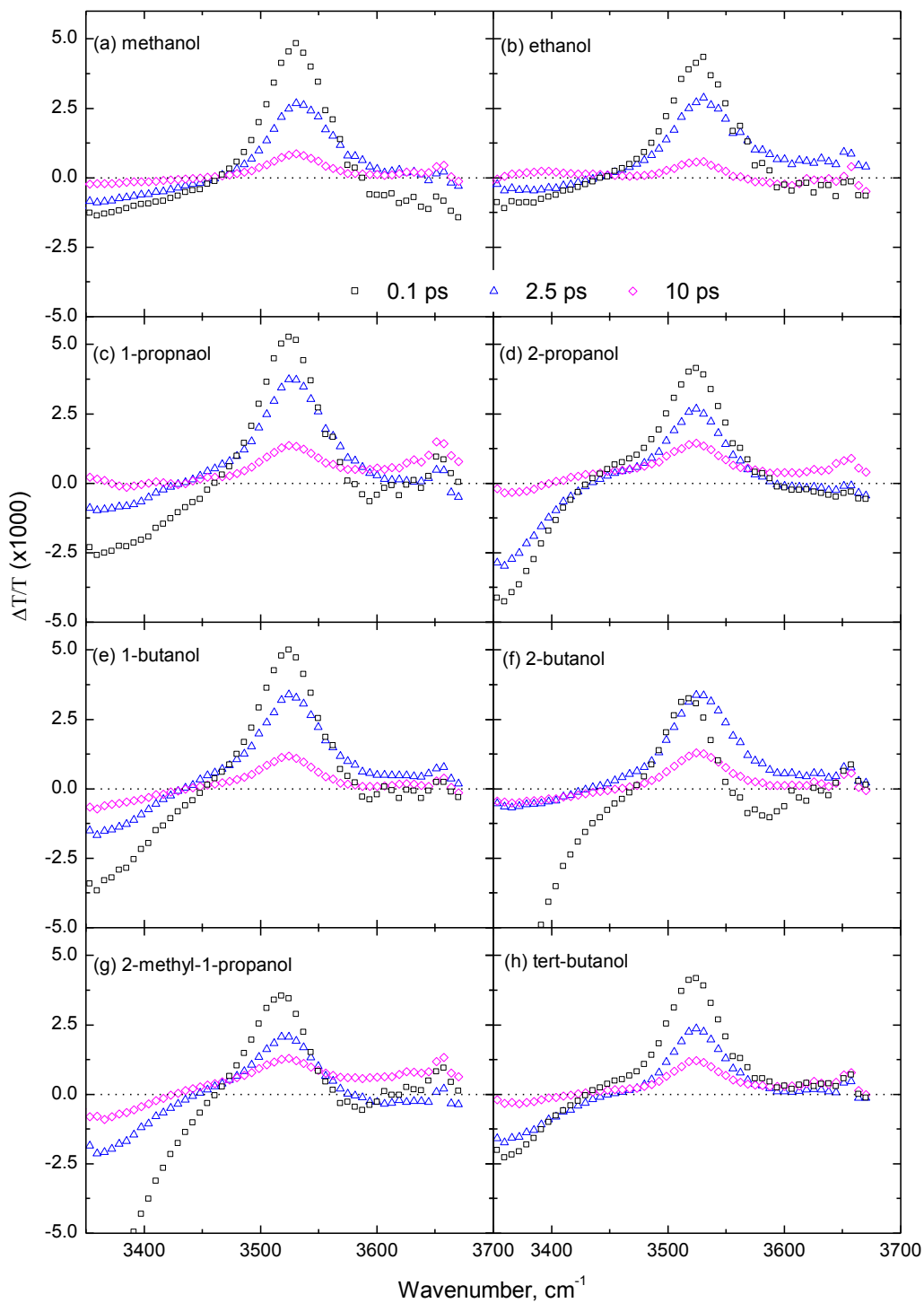


Fig. S6 Isotropic pump-probe transient spectra at different delay times (shown in the legend) for (a) methanol, (b) ethanol, (c) 1-propanol, (d) 2-propanol, (e) 1-butanol, (f) 2-butanol, (g) 2-methyl-1-propanol and (h) tert-butanol dissolved in MeCN.

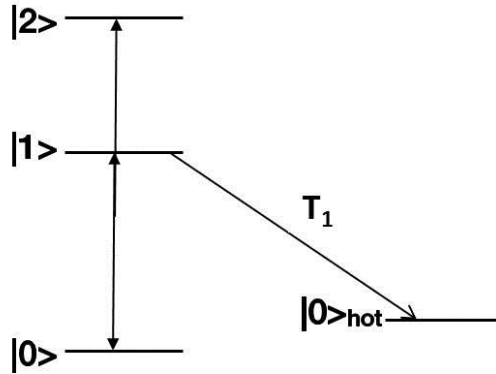


Fig. S7 Energy level diagram for the three-level kinetic model³. The excited $|1\rangle$ state of the OH-stretching mode relaxes to the hot ground state $|0\rangle_{\text{hot}}$, which corresponds to the temperature increase in the excitation volume at long times.

The pump-probe spectra, measured at short delay time and long delay time (Fig. S6, black and magenta symbols, respectively) substantially differ from each other. Such behavior is usually associated with the population relaxation to the “hot” ground state (Fig. S7) where the deposited into the OH stretch IR energy causes a temperature jump in the local volume due to energy redistribution among low-frequency collective modes.^{4,5} To extract the OH stretch lifetime T , the pump-probe data for each alcohol was fit with the following function:

$$S(\omega, t) = \left[A(\omega)e^{-\frac{t}{T}} + B(\omega) \left(1 - e^{-\frac{t}{T}} \right) \right] \quad (\text{Eq. 1})$$

convoluted with a Gaussian apparatus function of ~ 100 fs width. Here, $A(\omega)$ is the spectral profile of the population contribution represented by a sum of two Gaussian functions:

$$A(\omega) = A_{01} \exp \left[-\frac{(\omega - \omega_{01})^2}{2\sigma_{01}} \right] + A_{12} \exp \left[-\frac{(\omega - \omega_{12})^2}{2\sigma_{12}} \right] \quad (\text{Eq. 2})$$

where A_{01} and A_{12} , ω_{01} and ω_{12} , σ_{01} and σ_{12} are the local parameters, stand for the amplitude, frequencies and widths of the 0-1 and 1-2 transitions, respectively. $B(\omega)$ is the spectral profile of the thermal contribution that was also represented by an *ad hoc* combination of two Gaussians and a baseline.

The model described above was used to derive the lifetime of the OH-stretching mode and the timescale of the thermalization effect (~ 20 ps). Therefore, the 2D IR spectra at waiting times shorter than 5 ps have a negligible thermal contribution.

S5. Temperature jump in the hot ground state

To estimate the temperature jump, the linear absorption spectra of the studied solutions were measured at different temperatures and their difference was compared with the transient absorption spectrum at the delay time of 10 ps (Fig. S8). The temperature jump was estimated as ~ 0.3 - 0.5 K. Calculations based on the direct conversion of the absorbed pump energy (~ 0.9 μJ) into heat in the focal volume of $\sim 4 \cdot 10^{-7}$ cm^3 (the beam waist of ~ 100 μm , the jet thickness of 50 μm) resulted in the temperature jump of ~ 0.9 K.

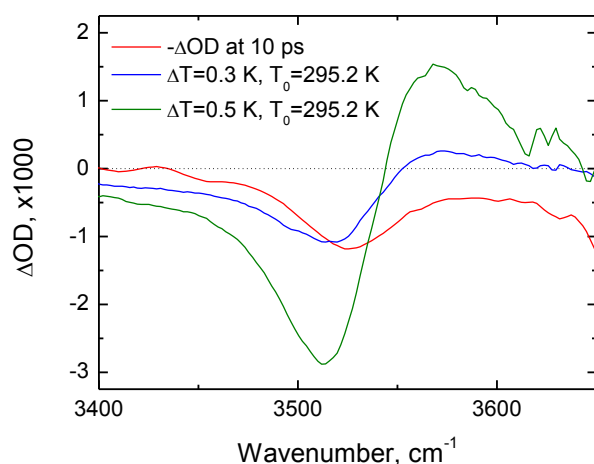
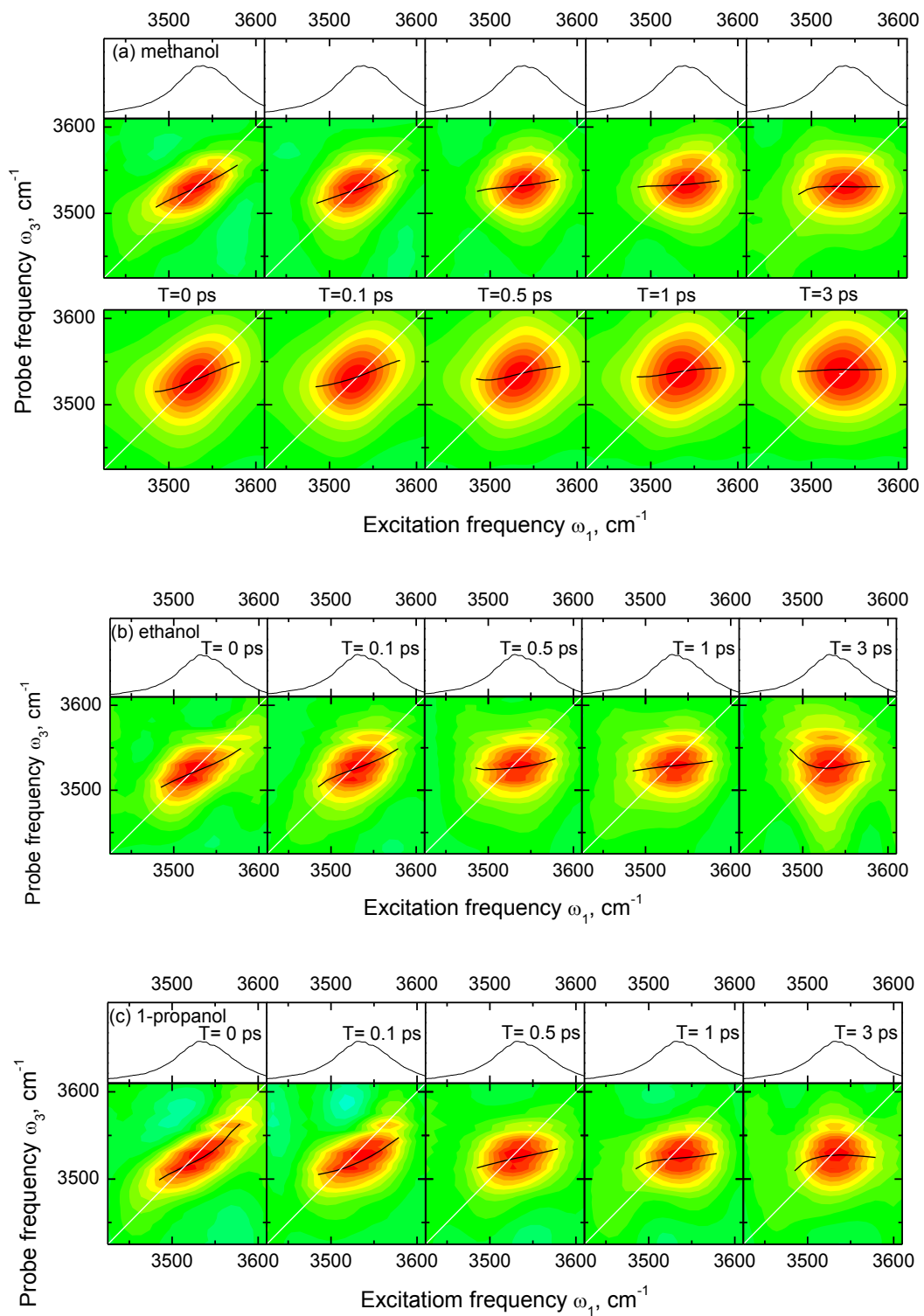
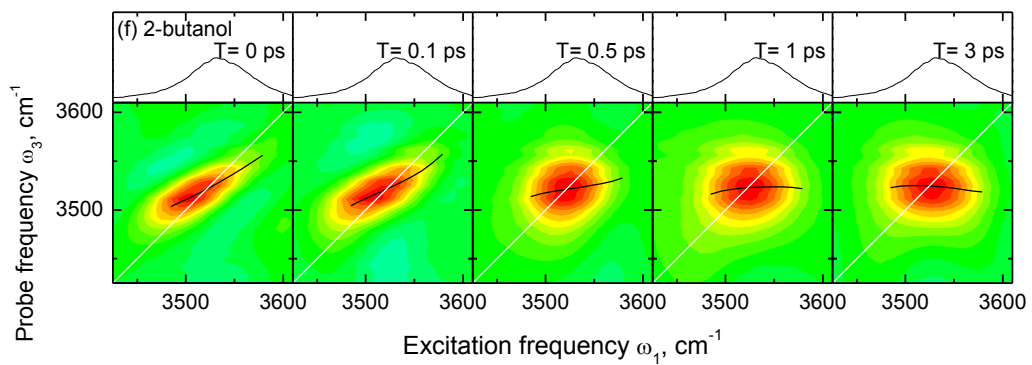
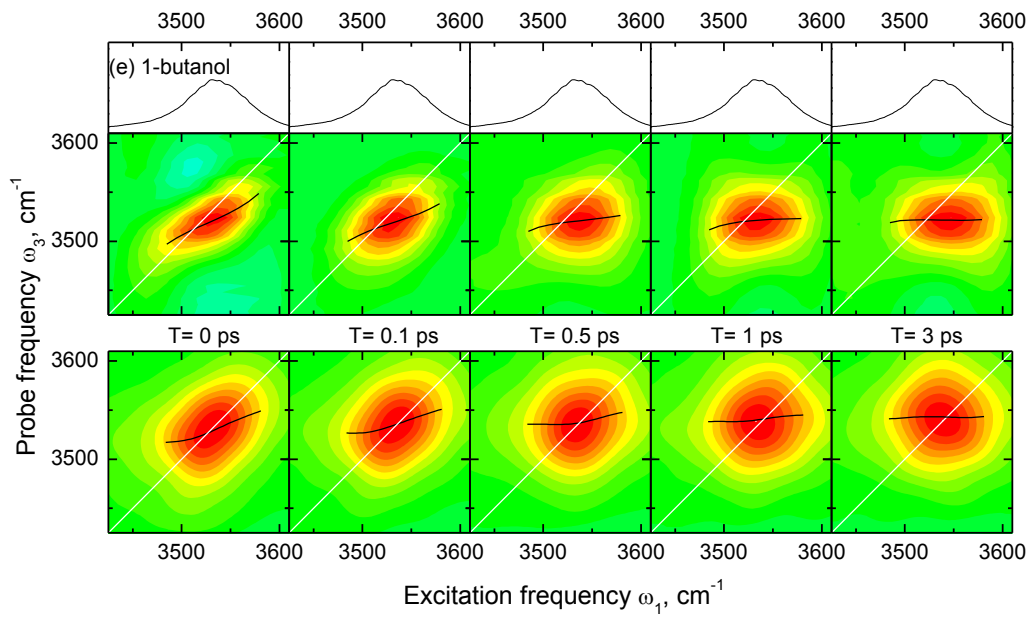
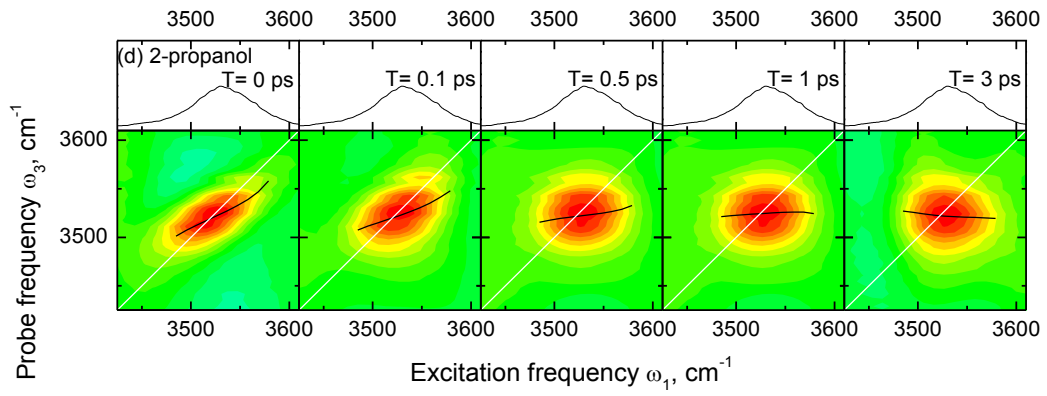


Fig. S8 The difference absorption spectra of 1-propanol/MeCN solution at two temperatures (blue and green lines) and experimental pump-probe spectrum at the delay of 10 ps (the red line).

S6. 2D IR spectra

2D IR spectra for all alcohols (in comparison with the experimental ones, if applicable) at a few waiting times of 0 ps, 0.1 ps, 0.5 ps, 1 ps and 3 ps are shown in Fig. S9. The 2D IR spectra are similar for all alcohols: at short waiting times the correlation between excitation and probing frequencies is high and, as the result, the 2D IR spectra are diagonally elongated. Increasing of the waiting time leads to the correlation loss which makes the shape of the spectrum to change to more round-like.





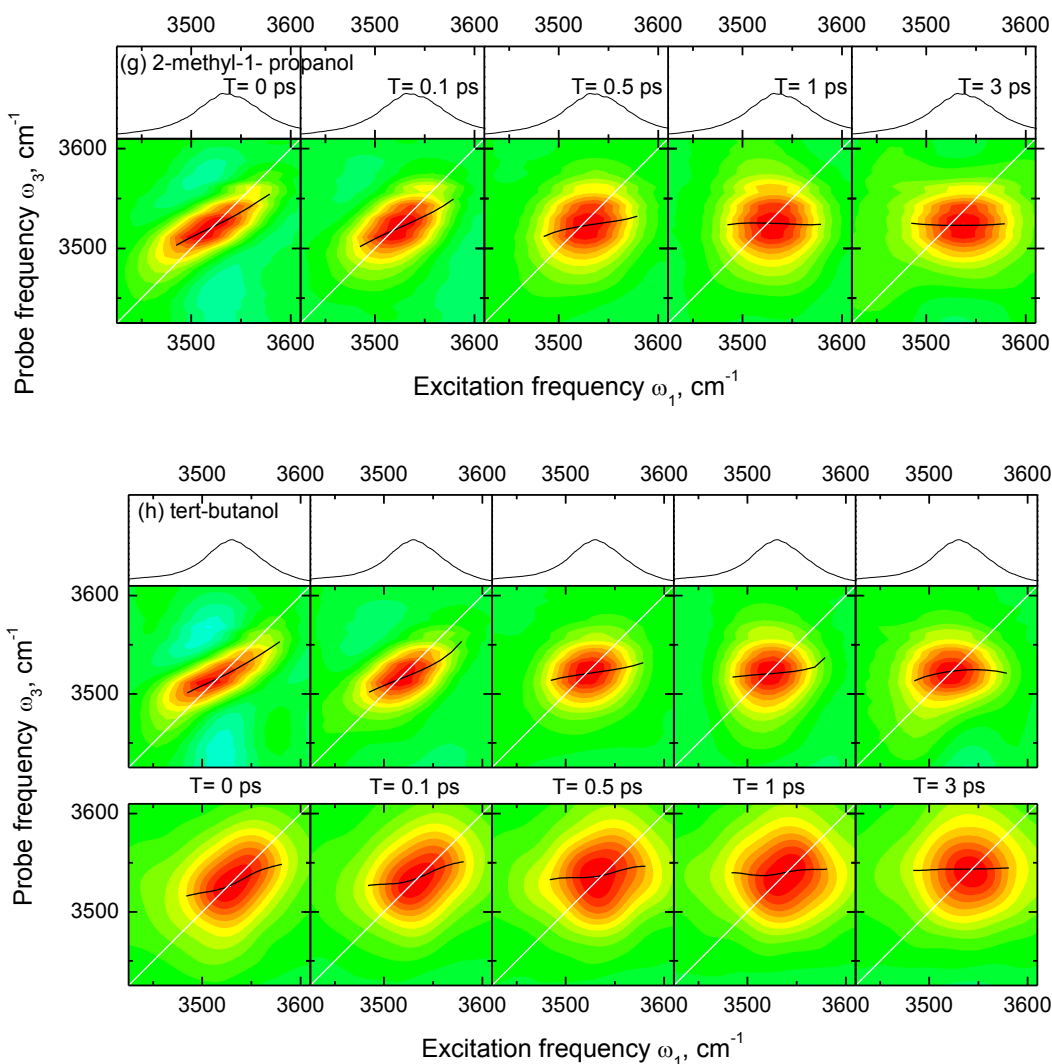


Fig. S9. Experimental absorption spectra (top panels), experimental (middle panels) and simulated (bottom panels, if applicable) 2D IR spectra in the OH-stretching mode region for MeCN solution of (a) methanol, (b) ethanol, (c) 1-propanol, (d) 2-propanol, (e) 1-butanol, (f) 2-butanol, (g) 2-methyl-1-propanol and (h) tert-butanol at a few representative waiting times. The 2D spectra are normalized to the maximal amplitude; only the bleaching region is shown. The equidistant contours are drawn with a 10% step of the maximal amplitude. The results of the CLS analysis are depicted by black lines. The simulated spectra (if applicable) are blue-shifted by 50 cm^{-1} along both axes for ease of comparison.

S7. Center Line Slope analysis

To extract the system-bath frequency-frequency correlation function, the center line slope (CLS) analysis⁶ was applied in OH-stretching mode region ($3485\text{--}3580 \text{ cm}^{-1}$, thick black lines in Fig. S9). Figures S10 and S11 show the results of the CLS analysis for individual alcohols and all alcohols, respectively. To extract the time scales, the obtained CLS dynamics were fitted with bi-exponential functions (see Fig. S12 for their parameters). All alcohols show similar behavior with no dependence on the size of alkyl chain group. The following timescales are obtained from the fit to the CLS data:

the fast one amounts to ~ 200 fs ($\sim 80\%$ share) and the slow one of ~ 4 ps ($\sim 20\%$ share). With MD simulations at hand, the fast component was attributed to OH-librations while the slow one originates from diffusional motion of the molecule.

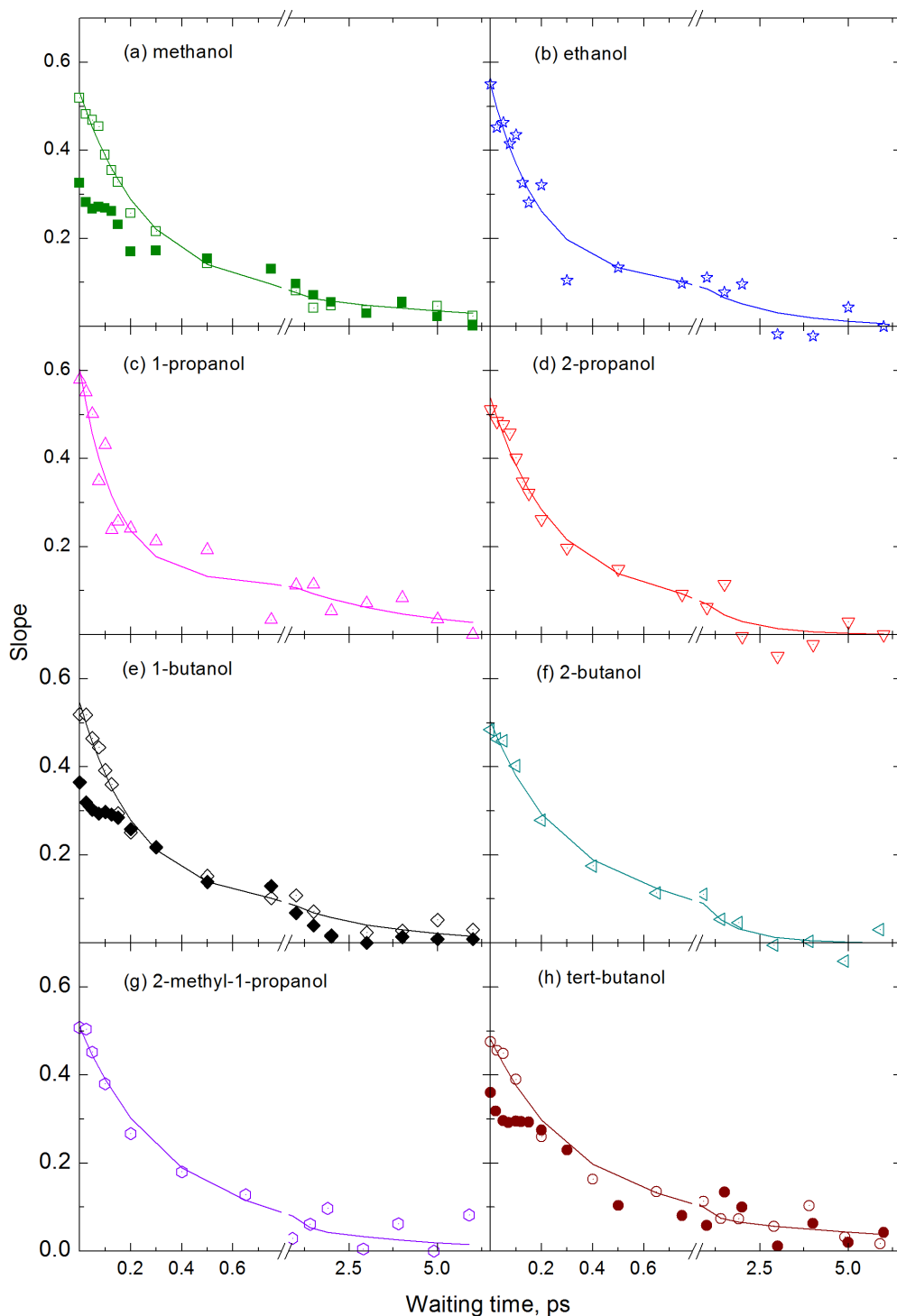


Fig. S10 Center line slope analysis, obtained from experimental 2D IR spectra for all studied alcohols: (a) methanol, (b) ethanol, (c) 1-propanol, (d) 2-propanol, (e) 1-butanol, (f) 2-butanol, (g) 2-methyl-1-propanol, (h) tert-butanol, obtained from experimental 2D IR spectra. The values of central line slope analysis, obtained from MD simulations for (a) methanol, (e) 1-butanol and (h) tert-butanol, are shown by filled symbols. Biexponential fits are shown by the solid lines; their parameters are summarized in Fig. S11.

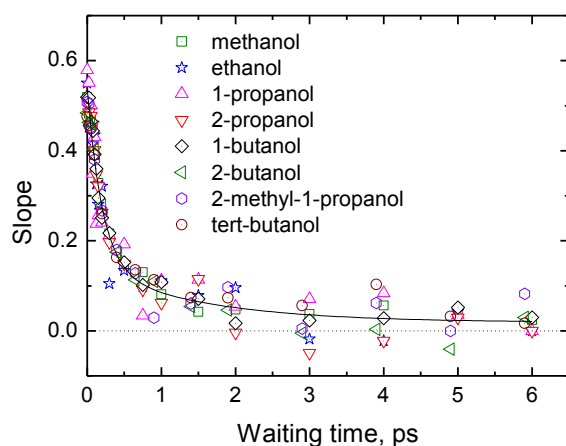


Fig. S11 The same as in Fig. S10, but all CLSs are depicted altogether. The averaged biexponential fit is shown by the thin black line.

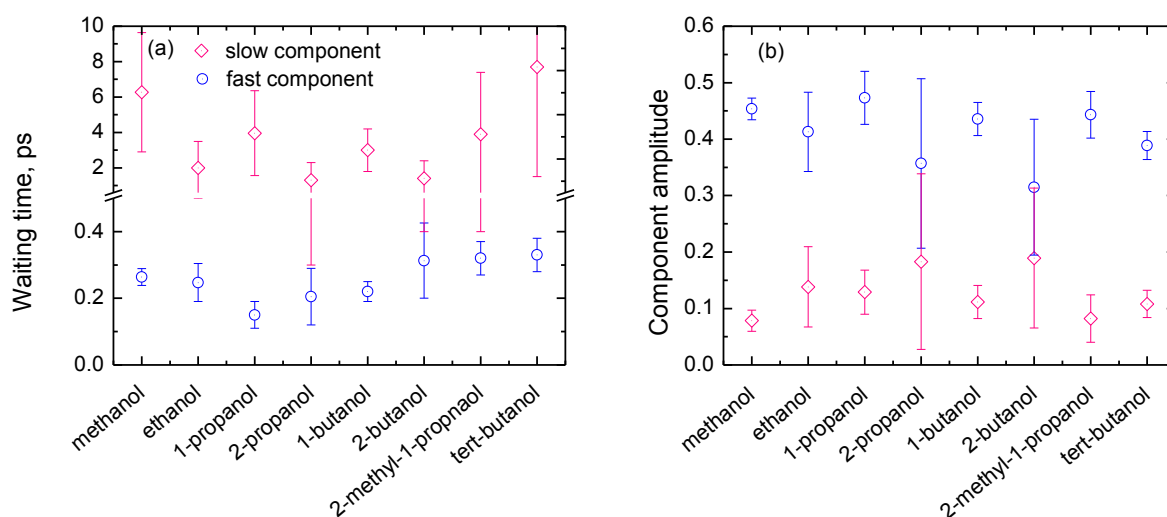


Fig. S12 Parameters of the biexponential fits to the CLS dynamics (Fig. S10). (a) decay times, (b) amplitudes.

References

- 1 S. S. Farwaneh, J. Yarwood, I. Cabaço and M. Besnard, *J. Mol. Liq.*, 1993, **56**, 317–332.
- 2 K. Shinokita, A. V. Cunha, T. L. C. Jansen and M. S. Pshenichnikov, *J. Chem. Phys.*, 2015, **142**, 212450.
- 3 S. Ashihara, N. Huse, A. Espagne, E. T. J. Nibbering and T. Elsaesser, *J. Phys. Chem. A*, 2007, **111**, 743–746.
- 4 J. B. Asbury, T. Steinel, C. Stromberg, K. J. Gaffney, I. R. Piletic and M. D. Fayer, *J. Chem. Phys.*, 2003, **119**, 12981–12997.
- 5 S. Yeremenko, M. S. Pshenichnikov and D. A. Wiersma, *Phys. Rev. A*, 2006, **73**, 21804.
- 6 K. Kwak, S. Park, I. J. Finkelstein and M. D. Fayer, *J. Chem. Phys.*, 2007, **127**, 124503.